Available on CMS information server

CMS AN -2009/041

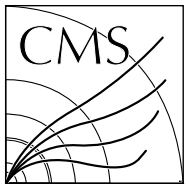

The Compact Muon Solenoid Experiment

Analysis Note

The content of this note is intended for CMS internal use and distribution only

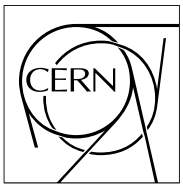

21 March 2009

Data-driven methods to estimate the electron and muon fake contributions to lepton analyses

W. Andrews, D. Evans, F. Golf, J. Mülmenstädt, S. Padhi, Y. Tu, F. Würthwein, A. Yagil

University of California, San Diego

C. Campagnari, P. Kalavase, D. Kovalskyi, V. Krutelyov, J. Ribnik

University of California, Santa Barbara

L. Bauerdick, I. Bloch, K. Burkett, I. Fisk, O. Gutsche

Fermi National Accelerator Laboratory, Batavia, Illinois

Abstract

This note presents two data-driven methods to estimate the QCD lepton fake contribution to di-lepton analyses. These methods are targeted to predict the fake contribution to the prompt isolated lepton signatures of WW and $t\bar{t}$ events. Only primary W/top/Z decay leptons are considered as true leptons. All other reconstructed leptons are considered fake. One method is based on the measurement of a ratio of very loose to tight selected leptons. This *fake rate* is extracted in bins of η and p_T to absorb phase space variations. Closure and validation tests are performed. They show that the fake prediction is in good agreement with actual observed fake contributions. The other method uses an extrapolation of isolation distributions from sideband regions to the signal region. This method also finds agreement with observed fake contributions.

1 Introduction

The purpose of this note is to present two data-driven methods to estimate the QCD electron and muon fake contributions to di-lepton analyses[1)].

The analyses currently considered are WW [1] and $t\bar{t}$ [2] in the di-lepton final state. Both analyses require events with missing transverse energy ($\not\!\!E_T$) to suppress Drell-Yan events. The main expected non-signal contributions to these analysis selections are W+jets, $t\bar{t}$ (for WW), remaining Drell-Yan and other di-boson processes such as WZ and ZZ.

In the context of these analyses, only primary W/top/Z decay leptons are considered as true leptons. All other reconstructed leptons are considered fake. For example on top of instrumental lepton fakes, also leptonic bottom and charm decays and leptons from conversions are considered fakes.

For the $WW/t\bar{t}$ selection the W+jets process is the dominant source of "fake background". The presented methods provide predictions for this background. The typical fake di-lepton signature from this process consists of one real lepton from the W decay and one fake lepton from a jet mis-identified as either an electron or a muon. The case of double fakes is much smaller and is not considered for now.

Firstly, a method is introduced which is based on the measurement of a ratio of very loose to tight selected leptons called *fake rate*. This method is referred to as *fake rate method*. The second method uses an extrapolation of isolation distributions from sideband regions to the signal region and is referred to as *sideband method*.

This note is organized as follows:

Section 2 introduces the main sources of fake leptons.

Section 3 introduces the overall concept of the fake rate method

Section 4 presents the determination of fake rates for selected electrons and muons (specifically for the given WW selection).

Section 5 describes the procedure of estimating the fake lepton contribution to a lepton signal selection using the fake rate method.

Section 6 describes tests performed to validate the fake rate method to predict fake leptons by performing:

- a closure test on the same sample used to determine the fake rates. This test is implemented to ensure absence of technical problems in the implementation of the method.
- a test on a sample with different physics content than the one from which the fake rate was determined. The fake rates are determined on inclusive QCD MC and tested by predicting the observed fakes in a W+jets MC sample. This is performed for both electrons and muons.
- a test of the systematic variation of the fake prediction when using different background samples enriched in varying physics content. For now, this is only a description of the planned procedure on real data.

Section 7 introduces the sideband method.

Section 8 describes the estimation of fake electrons using the sideband method.

Section 9 describes the estimation of fake muons again for the sideband method.

Section 10 tests the sideband method by applying it to the WW selection.

Section 11 concludes.

2 Origin of Fake Leptons

The fake contribution to a di-lepton final state depends strongly on the individual lepton selections.

The detailed lepton selection of the WW analysis used as a template for this note is described in App. A.

Leptons from Ws and tops are isolated and prompt. The main lepton selection cuts for the WW and $t\bar{t}$ analysis are:

[1)] When referring to leptons only electrons and muons are considered

- **High transverse momentum:** $p_T > 20$ GeV
- **Prompt:** coming from the primary vertex with small impact parameter
- **Isolated:** not surrounded by other tracks or neutral energy (other than accidental overlap with the soft underlying event)

In the following, we list the main sources of fake leptons for the above signal selection.

2.1 Electron fakes

There are several sources of backgrounds to the prompt isolated electron signature, (almost) all of which tend to be buried inside jets, and are thus reduced by isolation requirements:

- **Charge exchange interactions of charged pions:** As a charged pion turns into a neutral pion via charge exchange, the neutral pion decays to two photons. The entire energy of the charged pion is thus deposited in the calorimeter. The result is a track and an ECAL deposit with perfect E/p and impact parameter consistent with the primary vertex.
- **Fake electrons from photon conversion:** Any photon can convert early and asymmetrically and lead to a signal electron. Electrons from conversions tend to have impact parameters, inconsistent with the primary vertex.
- **Leptons from heavy flavor decays:** As only prompt leptons from $WW/t\bar{t}$ are considered signal, these leptons are considered fake.
- **matching ambiguity:** a photon cluster in the electromagnetic calorimeter is matched to a random track.
- **Final State Radiation (FSR) followed by conversions**: The tails of the FSR distribution in both energy and distance from the lepton may result in isolated electrons from conversion of the FSR photon.

The bulk of these fake contributions do not meet the lepton selection criteria. Background events passing the selection are rare events in the tails of e.g. isolation and impact parameter distribution.

2.2 Muon fakes

There are several sources of backgrounds to the prompt isolated muon signature:

- **Muonic Kaon and pion decays in flight:** Charged Kaons and pions have long lifetimes, but still have a finite probability to decay within the tracker volume before they reach the calorimeter or inside the calorimeter before they interact ($c\tau$ of 3.7 and 7.8 m, respectively).
- **Leakage of hadronic showers:** Hadronic interactions produce showers of varying depth, which logarithmically increases with hadron energy. In particular for high energy jets, there is a small but finite probability that one of the shower particles "leaks" out of the back of the calorimeter, and is detected in the inner muon chambers.
- **Sail through of hadrons:** There is a very small, but finite probability that a hadron will not interact at all before it stops or leaves the detector. In this case the hadron appears as a minimum ionizing particle, and is indistinguishable from a muon.
- **Cosmic ray muons:** A single cosmic ray muon crossing the detector close to the vertex region can be misreconstructed as two oppositely charged muons originating from the same vertex or even just a single muon, when one of the two legs is too much out of time to be recorded.
- **Matching ambiguities:** Non-muon tracks from the central tracking system can be accidentally associated to muon system hits or tracks produced by either a true muon or a background "muon" from one of the other background categories above.
- **Leptons from heavy flavor decays:** As for electrons.

3 Fake Rate method

3.1 General approach

The goal is to estimate the fake lepton contribution to a signal lepton selection. This estimate is derived from data only and thus does not rely on MC simulation.

The method consists of a determination and an application part where both parts use statistically independent data samples. In the determination part, an inclusive jet trigger is used to select a fake dominated background sample. This sample is used to measure the fraction of signal leptons *(numerator)* to looser-defined leptons *(denominator)* called the *fake rate*. This fake rate is expected to vary within the considered phase space, therefore it is extracted in bins of η and p_T of the fake leptons.

In the application part, the fake contribution to the signal sample triggered by single leptons is estimated by weighting the denominator leptons contribution with the fake rate.

The above fake rate is not an absolute lepton fake rate. It is only valid for a specific numerator and denominator selections:

- The numerator is determined by the analysis lepton selection,
- The choice of the denominator is un-constrained and is usually the key to accuracy and stability of the procedure.

The denominator is chosen to be stable against varying physics content (e.g. heavy flavor contribution) and kinematical variations (e.g. jet E_T, rapidity dependence) within the η and p_T bins of the fake rate.

In the following, separate fake rates for electrons and muons are determined.

4 Fake Rate Determination

4.1 Electron Fake Rate Determination

The denominator and numerator selections for the electron fake rate are based on the GSF electron collection. Table 1 lists the selection cuts for the denominator and numerator.

Cut	**Denominator**	**Numerator**
transverse momentum	$p_T^e \geq 20$ GeV	$p_T^e \geq 20$ GeV
pseudo rapidity	$\lvert\eta_e\rvert \leq 2.5$	$\lvert\eta_e\rvert \leq 2.5$
closest muon veto	$\Delta R_{e-\mu} > 0.1$	$\Delta R_{e-\mu} > 0.1$
had/elmag energy fraction	$H/E \leq 0.2$	included in electron identification
track based isolation, see B.1	$p_T^e/(p_T^e + tkIso) > 0.92$	
track+calo based isolation, see B.2	$p_T^e/(p_T^e + sumIso) > 0.75$	$p_T^e/(p_T^e + sumIso) > 0.92$
impact parameter		$\lvert d_0^e\rvert \leq 0.025$
electron identification		Tight electron ID (see App. F and [1])

Table 1: Electron numerator and denominator selection based on GSF electron collection.

This definition relaxes the electron isolation and identification cuts as well as the impact parameter cut in the denominator. These cuts result from a simple optimization on low statistics MC. They might have to be revisited in the light of data.

In the absence of data, an inclusive PYTHIA QCD MC sample (see App. C) is used to simulate the inclusive background sample. The available statistics is of the order of 1 pb^{-1}. As soon as data is available, an inclusive single jet trigger data sample will be used. Then, to remove biases introduced by this jet trigger, only denominator or numerator objects which are outside a cone of $\Delta R < 0.2$ of the leading jet will be considered.

A two-dimensional fake rate in η and p_T of the leptons is extracted after the trigger bias pre-selection.

The last p_T bin of the fake rate is used for $p_T^e > 150$ GeV.

The resulting 2D fake rate and their 1D projections in η and p_T including their binomial errors can be seen in Fig. 1. The fake rate is found to be symmetric in η within the errors. Therefore, the available statistics was increased by considering each numerator and denominator object symmetrically at $\pm|\eta|$.

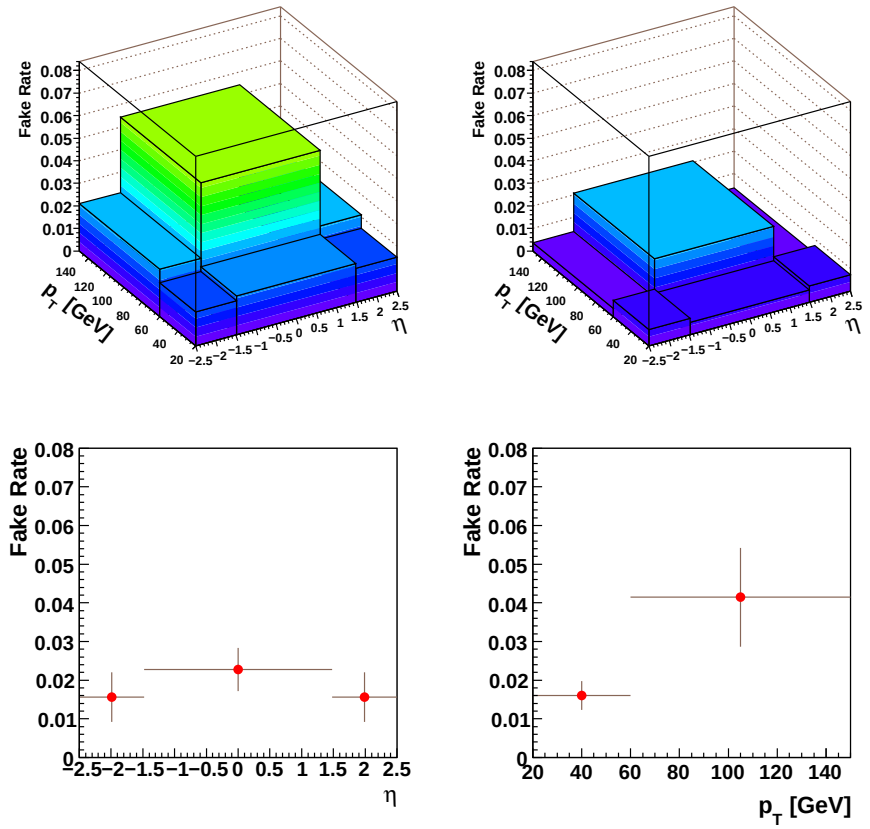

Figure 1: Electron fake rate extracted from QCD samples (symmetrized in $|\eta|$). *Top left*: 2D fake rate, *top right*: 2D fake rate binomial error, *bottom left*: 1D projection of fake rate in η, *bottom right*: 1D projection of fake rate in p_T.

The average electron fake rate is $\approx 2\%$ and it varies from $\approx 1.2\%$ to $\approx 5.5\%$ in all bins. The error varies between $\approx 0.4\%$ and $\approx 2\%$.

As a side: the current fake rate binning is very coarse due to the lack of statistics. It is planned to increase the number of bins when more statistics in MC or data becomes available.

4.2 Muon Fake Rate Determination

In analogy to the electron fake rate determination, the denominator and numerator selections for the muon fake rate are based on the global muon collection. Table 2 lists the selection cuts for the denominator and numerator.

Cut	**Denominator**	**Numerator**
transverse momentum	$p_T^\mu \geq 20$ GeV	$p_T^\mu \geq 20$ GeV
pseudo rapidity	$\lvert\eta_\mu\rvert \leq 2.5$	$\lvert\eta_\mu\rvert \leq 2.5$
track+calo based isolation, see B.2	$p_T^\mu/(p_T^\mu + sumIso) > 0.75$	$p_T^\mu/(p_T^\mu + sumIso) > 0.92$
number of tracker+μ-chamber hits		$n_{Hits} \geq 11$
global μ fit:	$\chi^2/NDoF \leq 20$	$\chi^2/NDoF \leq 10$

Table 2: Muon numerator and denominator selection based on global muon collection.

This definition relaxes the muon isolation and identification cuts in the denominator.

The muon fake rate is determined following the same steps as for the electrons on the same PYTHIA QCD MC sample (see App. C) corresponding to order of 1 pb^{-1}. The resulting 2D fake rate and their 1D projections in η and p_T including their binomial errors can be seen in Fig. 2. Also here, the available statistics was increased by considering each numerator and denominator object symmetrically at $\pm|\eta|$.

The average muon fake rate is $\approx 10\%$ and it varies from $\approx 1\%$ to $\approx 25\%$ in all bins. The error varies between

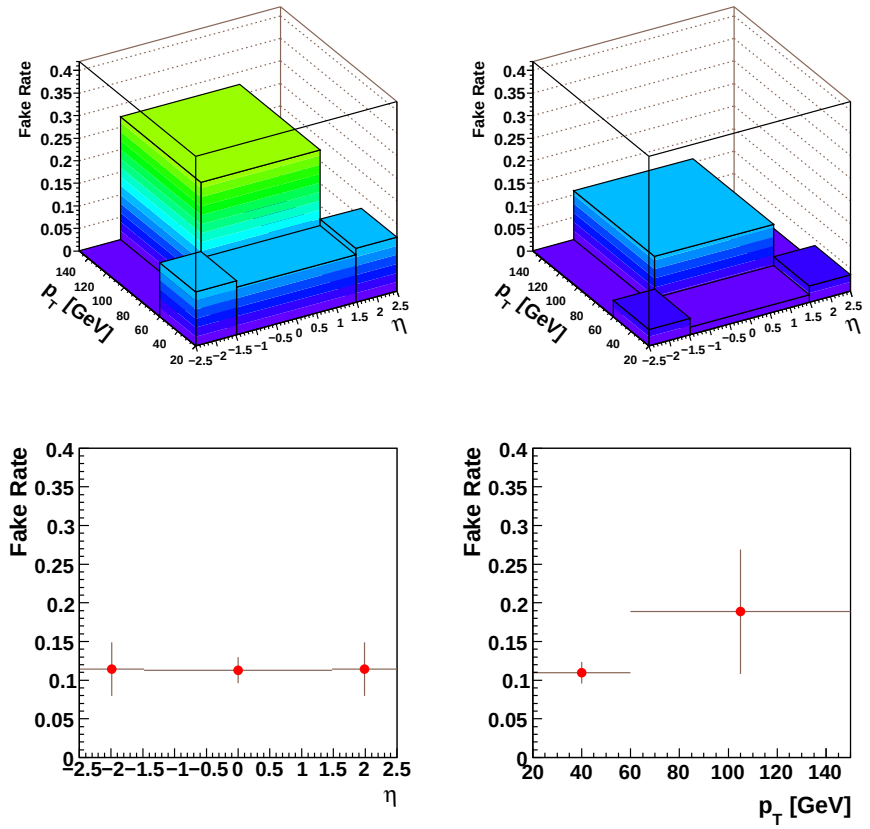

Figure 2: Muon fake rate extracted from QCD samples (symmetrized in $\pm|\eta|$. *Top left*: 2D fake rate, *top right*: 2D fake rate binomial error, *bottom left*: 1D projection of fake rate in η, *bottom right*: 1D projection of fake rate in p_T.

$\approx 1\%$ and $\approx 10\%$.

5 Fake Rate Application

In the application part, the fake rates from Sec. 3 are used to estimate the fake contribution to the dilepton signal sample. The signal sample is pre-selected using single lepton triggers. The procedure to determine the fake contribution is described in the following:

1. Under the assumption that every analysis di-lepton contains at least one triggered lepton, all di-lepton candidates are selected where the triggered lepton fulfills the numerator cuts from Sec. 4.1.

2. The second lepton of the selected di-lepton candidate is required to fulfill the denominator selection and **not** the numerator selection. This removes a bias in the signal enriched samples introduced by the signal leptons.

3. Selected di-lepton candidates are then scaled with the following weight:

$$weight = \frac{FR(\eta^{den}, p_T^{den})}{1 - FR(\eta^{den}, p_T^{den})} \tag{1}$$

   where $FR(\eta^{den}, p_T^{den})$ is the entry from the two-dimensional fake rates from Sec. 3 at η and p_T of the denominator and not numerator lepton. For p_T larger than the last bin of the fake rates, the corresponding fake rate from the last p_T bin is used.

For the time being, the following simplifying assumptions are made and will be corrected for in a future high statistics scenario:

- Double fakes are neglected. This contribution is very small.

- No trigger treatment is performed so far. It is assumed that each reconstructed numerator lepton has triggered the event.

This procedure guarantees that an individual di-lepton candidate is only taken into account once. The error treatment of the application is described in App. D.

6 Fake Rate Validation

To evaluate the performance of the lepton fake prediction, different MC simulation samples are used to compare actual observed lepton fakes with predicted lepton fakes.

6.1 Closure test

A simple closure test is performed using the QCD MC samples described in App. C to ensure absence of technical problems in the implementation of the method. Two statistically independent MC sub-samples are extracted from the QCD samples by selecting events with even or odd event numbers. The determination uses even events while the application uses odd events.

The fake rates extracted from the even events of the QCD samples are comparable to the rates presented in Sec. 3 using the complete sample only with larger statistical errors.

The application to the odd events of the QCD samples uses a simplified version of the fake rate application procedure described in Sec. 5. Here, the observed fakes are all leptons fulfilling the numerator cuts. The estimated fakes are all leptons fulfilling the denominator cuts and **not** the numerator cuts weighted by Eq. 1.

Tab. 3 shows the comparison between observed and predicted electron fakes normalized to 1 fb^{-1}.

	fake electrons for 1 fb^{-1}
observed	927479 ± 176101
predicted	958151 ± 26822

Table 3: Comparison between observed and estimated electron fakes extracted from the odd events of the QCD samples.

Fig. 3 shows the comparison of observed and predicted fake electron p_T^e and η^e. The predicted electron fakes are consistent with the actual observed fake electrons. This proves the absence of technical problems.

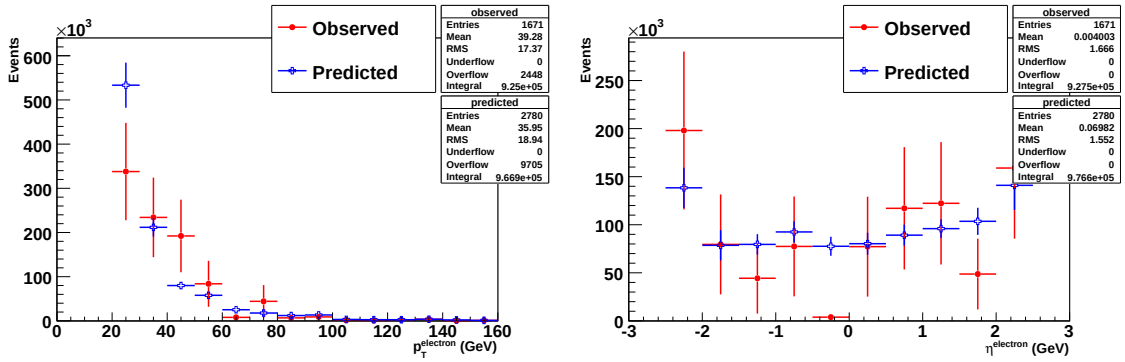

Figure 3: Closure test comparing observed and predicted electron fakes in QCD MC samples. *left*: p_T^e, *right*: η^e. Distributions are scaled to 1 fb^{-1}.

The corresponding test of the muon fake contribution is shown in Tab. 4.

	fake muons for 1 fb^{-1}
observed	527992 ± 137421
predicted	509499 ± 49321

Table 4: Comparison between observed and estimated muon fakes extracted from the odd events of the QCD samples.

The comparison of observed and predicted fake muon p_T^μ and η^μ is shown in Fig. 4. Also here, prediction and observation are consistent within the errors.

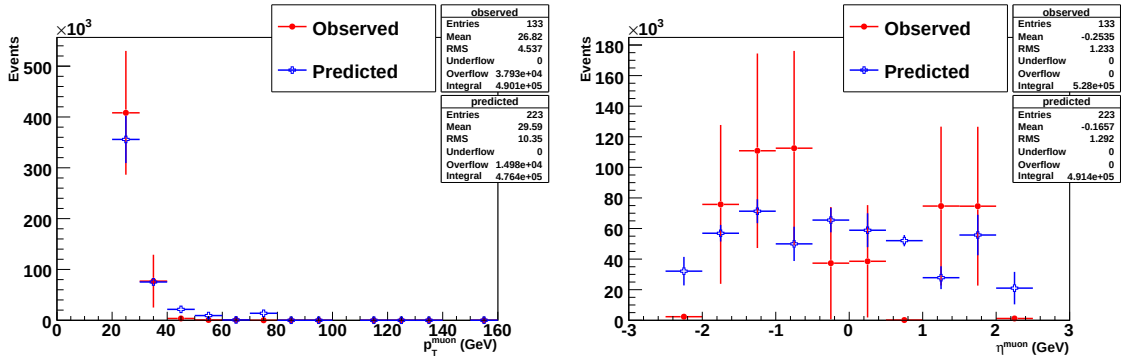

Figure 4: Closure test comparing observed and predicted muon fakes in QCD MC samples. *left*: p_T^μ, *right*: η^μ. Distributions are scaled to 1 fb^{-1}.

6.2 MC Application test

To test the fake rate method on a sample with different physics content, observed and predicted fake leptons are compared in W+Jets MC. This sample describes the dominant fake lepton background contribution to the WW and $t\bar{t}$ di-lepton analyses to which this procedure is targeted.

Following the procedure of the closure test and using the lepton fake rates determined from the QCD samples from Sec. 3, the W+jets sample is pre-selected by requiring a true lepton coming from the W to tag the real lepton of a possible di-lepton signature. Any additional lepton in these events is defined to be fake and treated in the same way as the leptons in the closure test in Sec. 6.1 to extract the predicted and observed fake contribution to the di-lepton signal. For simplicity, the comparison is constraint to the $e-\mu$ di-lepton final state.

There is however a subtlety in this procedure. Some of the $e-\mu$ di-lepton final state events in the used W+jets sample are coming from $W \to \mu\nu\gamma$ where the opening angle between the γ and the truth tagged μ is large. The γ converts asymmetrically and is then reconstructed as an electron. The extracted fake rate is not meant to reproduce these events. Thus, these events are identified at the generator level and removed from this test. The fraction of $e-\mu$ events in the W+jets sample that can be ascribed to this process is $\sim 36\%$.

The comparison between observed and predicted electron fakes in the W+jet sample is shown in Tab. 5.

	fake electrons for $1\ fb^{-1}$
observed	36.3 ± 13.7
predicted	37.8 ± 2.1

Table 5: Comparison between observed and estimated electron fakes extracted from the W+jets sample.

Fig. 5 shows this comparison for electron fakes in p_T and η of the electron. The predicted fake electrons are compatible with the observation.

The corresponding comparison for muon fakes is shown in Tab. 6 and Fig. 6. Also here prediction and observation are compatible with each other.

	fake muons for $1\ fb^{-1}$
observed	20.7 ± 10.4
predicted	14.5 ± 3.4

Table 6: Comparison between observed and estimated muon fakes extracted from the W+jets sample.

In addition, Fig. 7 shows the comparison of observed and predicted fake leptons differential in the number of jets in the event.

All comparisons suffer from significantly low statistics in the available W+Jets MC sample (Summer08/Fall08). The same comparison was also performed employing equivalent denominator and numerator selections on an older W+jets MC sample (CSA07) with significantly more statistics. This comparison shows very good agreement with

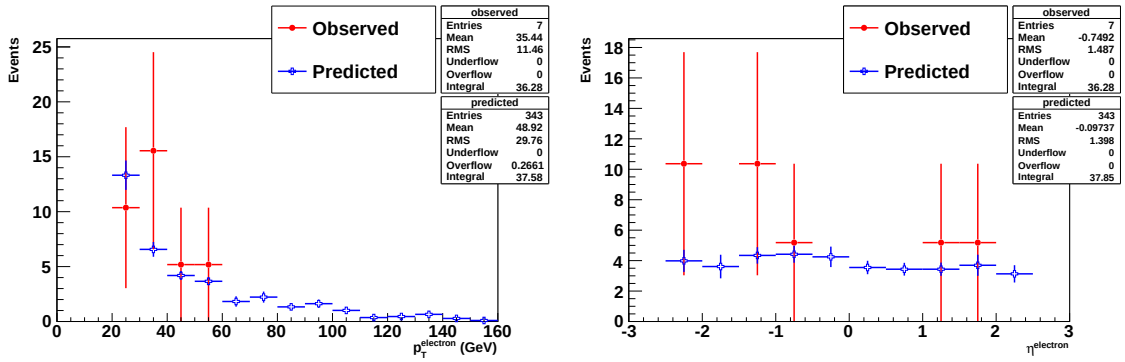

Figure 5: Application test comparing observed and predicted electron fakes in W+jets MC di-lepton events in the $e - \mu$ final state using fake rates extracted from QCD samples. *left*: p_T^e, *right*: η^e. Distributions are scaled to 1 fb^{-1}.

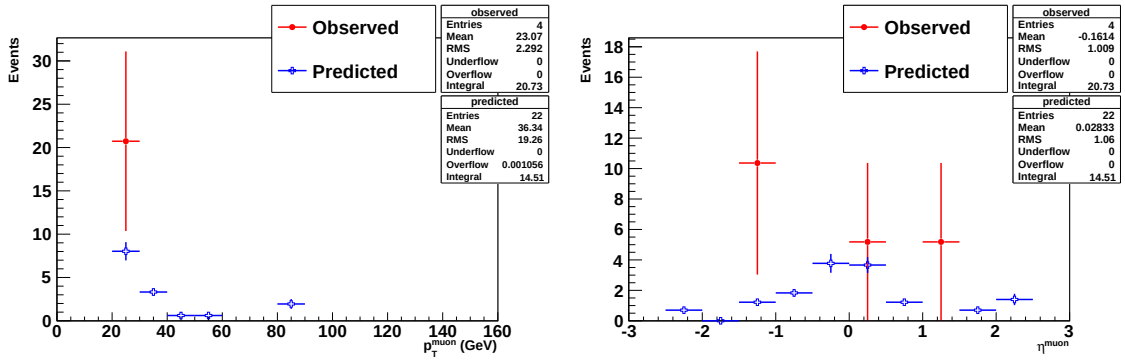

Figure 6: Application test comparing observed and predicted muon fakes in W+jets MC di-lepton events in the $e - \mu$ final state using fake rates extracted from QCD samples. *left*: p_T^μ, *right*: η^μ. Distributions are scaled to 1 fb^{-1}.

much higher significance between observation and prediction (see Fig. 8 and App. E).

These tests allow the conclusion that the fake rate method works in di-lepton final states and can be used to estimate the fake contributions to the WW and $t\bar{t}$ analyses.

Figure 18 shows the distribution in transverse momentum for the predicted and observed fake electrons using the CSA07 W+jets sample.

Once CMS has recorded collision data, fake rates will be determined in different data sets (e.g. on different jet trigger streams). The predictions obtained with these fake rates will be checked for consistency on several data samples. It is foreseen to follow the procedure described in [4] as sketched in the following.

6.3 Testing fake rate procedures in data

The MC test done in 6.2 is useful (and doable) for MC based and derived fake rate (as is done in this context). From our experiences we've learned that MC often fails to predict fake rates accurately. In this section we describe our plan to test and characterize the performance of our fake prediction using data.

We intend to determine the fake rate from one (or few) inclusive jet trigger(s). The derived fake rate is then to be applied to a variety of other test samples like inclusive photon, other inclusive jet triggers with different thresholds and pre-scales and so on. In applying this test, care must be taken to account for the genuine EWK contamination of the tested samples (for example, observe a Z signal in a di-jet sample, estimate the rate, correct the fake rate for it).

As the purpose is to test the robustness of the procedure against variation in kinematical conditions as well as physics content, we plan to do it by confronting the prediction based on the fake rate we derived to the observed number of events in different samples. This will serve both to validate the procedure as well as to determine its limitations and the systematic uncertainties associated with it.

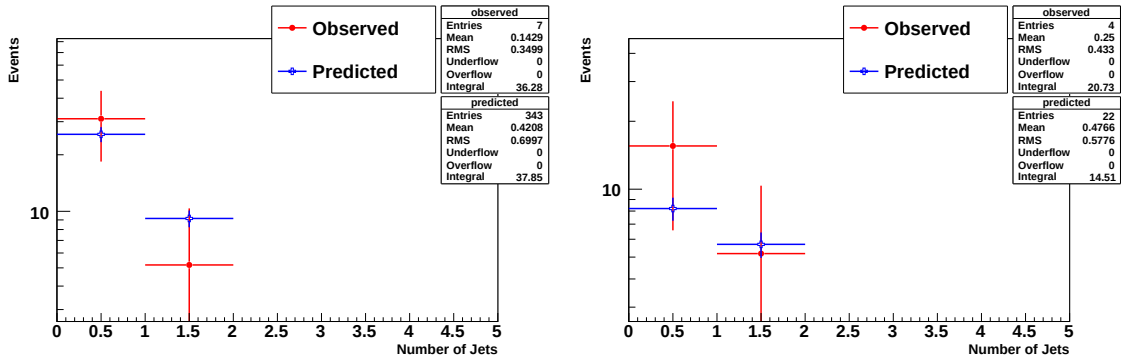

Figure 7: Application test comparing observed and predicted lepton fakes in W+jets MC di-lepton events in the $e - \mu$ final state using fake rates extracted from QCD samples differential in n_{jet}. *left*: electrons, *right*: muons. Distributions are scaled to 1 fb^{-1}.

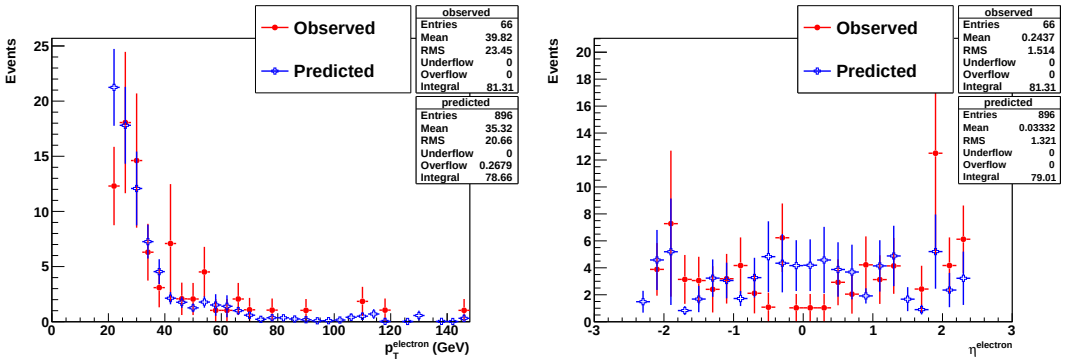

Figure 8: Application test comparing observed and predicted electron fakes in older W+jets MC di-lepton events in the $e - \mu$ final state using fake rates extracted from QCD samples produced using samples from an older MC production cycle (CSA07). *left*: p_T^e, *right*: η^e. Distributions are scaled to 1 fb^{-1}.

A similar strategy for testing lepton fake rates determined in collision data is outlined in [4].

7 Sideband Method

Lepton isolation is the main discriminating variable against fake leptons from jets. It is natural to expect that the number of fake leptons monotonically decreases with tighter isolation requirements. Extrapolating the isolation distribution to the isolated region, it is possible to estimate the remaining W+jets background contribution.

In order to make this idea work, we need to understand how well we can predict the shapes of the fake and true lepton isolation distributions. Given that a number of different background processes may contribute to the final selection, it is important to understand how different their isolation distributions are from the signal and W+jets background distributions. We also need to check for secondary sources of background events associated with W+jets, which may look signal-like in the isolation distribution.

8 Sideband Method: Fake Electrons

Fake electrons are dominated by charged pions depositing most of their energy in the ECAL, neutral pions producing electrons via internal or external conversion and electrons from semi-leptonic decays of heavy quarks. Figure 9 shows the fake electron isolation distribution of $W \rightarrow \mu\nu$ Monte Carlo simulated events, which were identified by the presence of a hard scatter muon (status 3) in the generator particle list. Electrons are required to be above 20 GeV p_T and pass the electron ID requirements. No explicit muon veto is applied at this point.

Among the major sources of fakes, only two components violate the assumption of monotonic decrease of the number of fake electrons with tighter isolation requirements: muons from W faking electrons (blue) and $W \rightarrow \mu\gamma\nu$ (magenta). Both these sources represent only one physics process: $W \rightarrow \mu\gamma\nu$. Most of these events can be effectively removed by requiring the absence of muons within $\Delta R = 0.1$ of the electron. Unfortunately such a

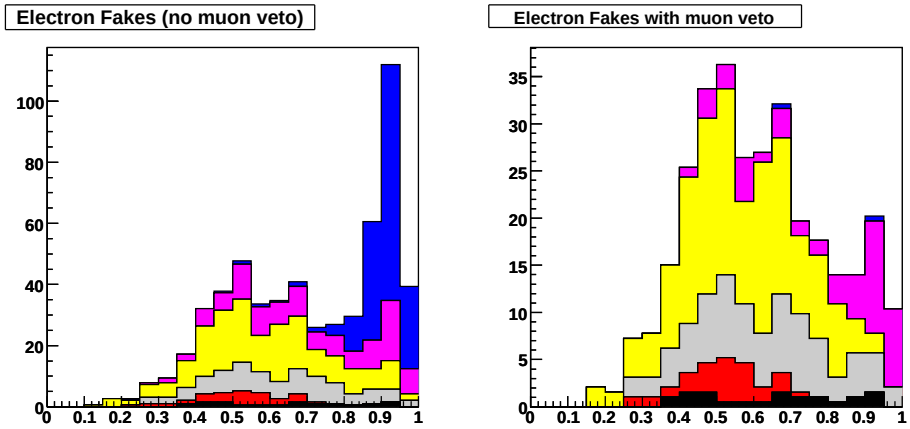

Figure 9: Shown are relative isolation distributions for the dominant sources of fake electrons for $W \to \mu\nu$ events: $\pi^0 \to \gamma ee$ (black), heavy quark semi-leptonic decays (red), conversion of photons from π^0 (grey), muons from W faking electrons (blue), $W \to \mu\gamma\nu$ (magenta), all others (yellow). Left: no explicit veto on muons is applied here. Right: electrons are required to be more than $\Delta R = 0.1$ away from muons. Events are weighted for $100pb^{-1}$ integrated luminosity at 10TeV.

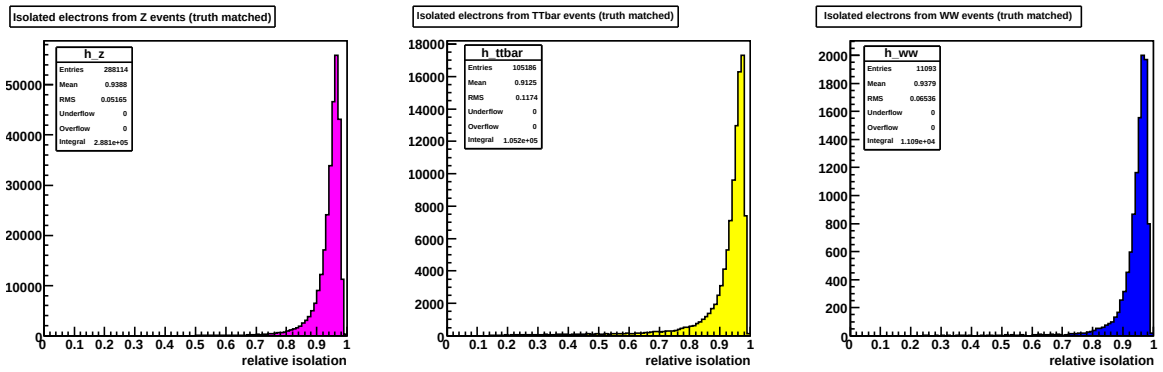

Figure 10: Shown are relative isolation distributions for isolated electrons from: $Z \to ee$ (magenta), $t\bar{t}$ (yellow), WW (blue) events. Electrons are truth-matched to come from vector bosons and have standard selection requirements. The scale is arbitrary.

veto does not remove all fakes of this type and $W \to \mu\gamma\nu$ events with the photon at large angle with respect to the muon may require special treatment. Fortunately the effect is suppressed by the requirements for the photon to convert and be isolated. So at 100 pb^{-1} the effect can be easily covered by the large statistical and systematic uncertainties and will have no impact on the final results.

The isolation distribution for real isolated electrons should look very similar for different sources since they are dominated by noise and the underlying event. Figure 10 shows isolation distributions for electrons from vector bosons for WW, $t\bar{t}$ and Z events. It is clear that these distributions are essentially identical and in real data we could use Z decays as a control sample. The large statistics and clean signature of $Z \to ee$ events allows us to get a pure sample of electrons to parameterize the isolated electron distribution from data.

Shapes of background isolation distributions may differ from sample to sample. Figure 11 shows the isolation distributions for electrons for different QCD samples. The significance of the variation of the shape of the distributions depends on the expected precision. If the integrated luminosity is significant, it should be possible to fit for the shape of the background distribution from data. Otherwise, the shapes can be extracted from QCD samples, taking the difference between various samples as systematic uncertainty.

Figure 12 shows the expected W+jets background contribution in the isolation region $[0.92, 1.0]$ for the $WW \to l\nu l\nu$ analysis (normalized to 100 pb^{-1}), fixing the background distribution to that of QCD samples. Taking the average of the results as the central value and half of the maximum difference as the systematic uncertainty, the expected W+jets background contribution in the signal region is 1.6 ± 0.4. It is important to estimate the $W \to \mu\gamma\nu$ contribution (e.g. using Monte Carlo predictions) to avoid an underestimation of the W+jets background in the

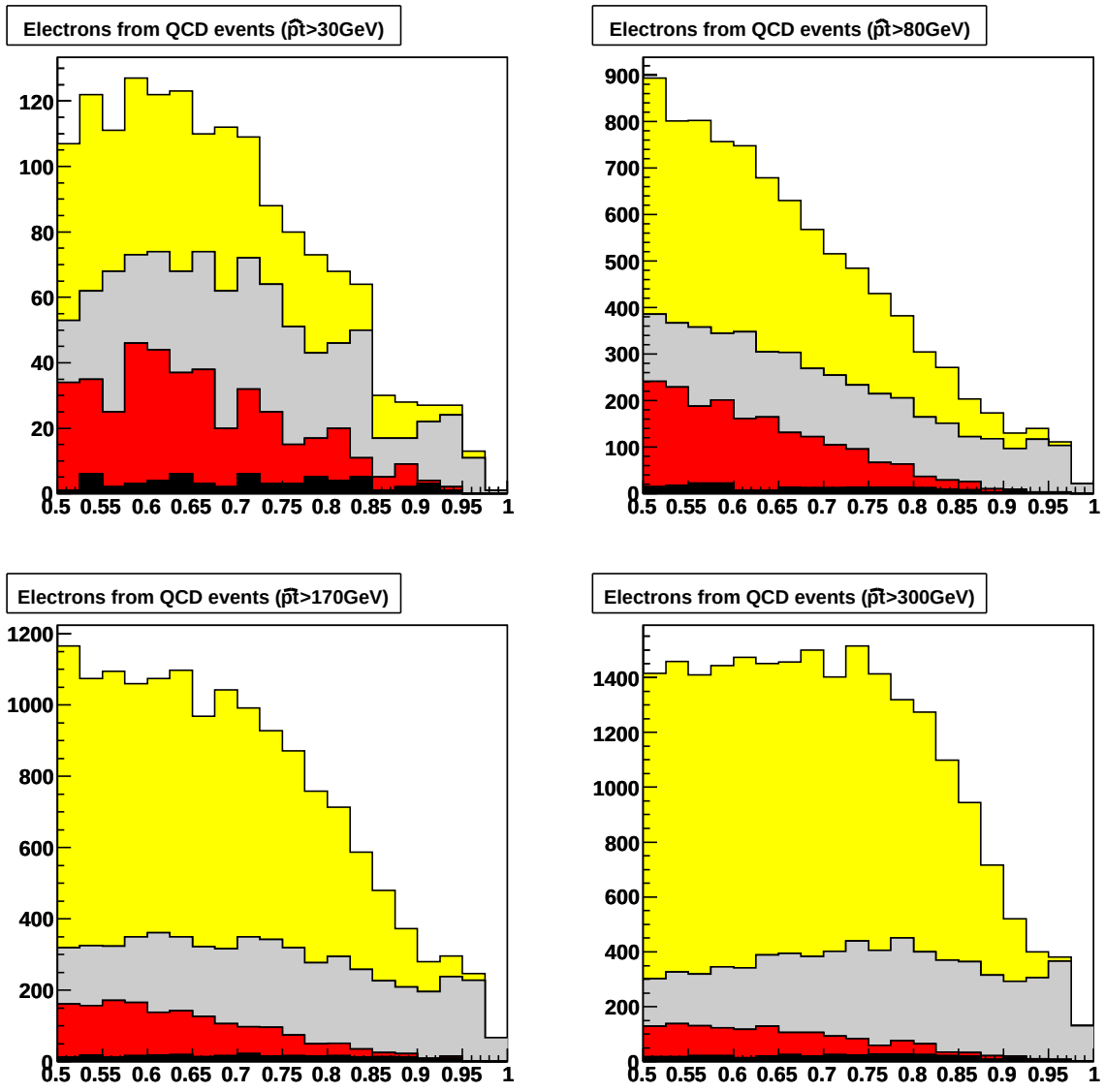

Figure 11: Shown are the relative isolation distributions for electrons in different QCD samples. Each distribution is split into 4 categories: $\pi^0 \rightarrow ee\gamma$ (black), electrons from heavy flavor decays (red), photon conversions (grey), and all other sources (yellow). The scale is arbitrary.

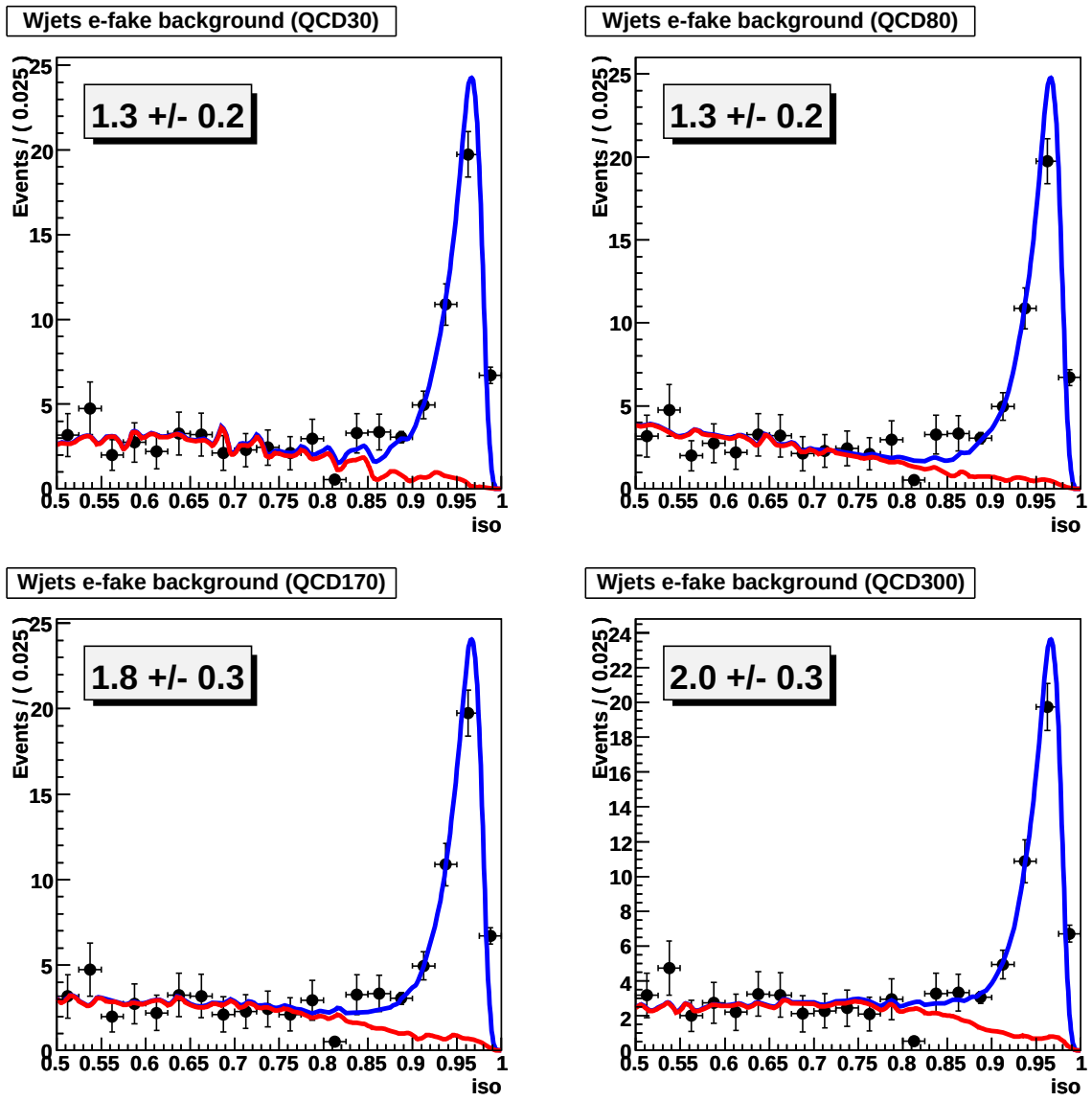

Figure 12: Unbinned maximum likelihood fits on the full sample of events. The signal pdf was extracted from $Z \rightarrow ee$ events. The background pdf was extracted from various QCD samples. The red curve represents the background distribution. The W+jets background estimates due to fake electrons in the region $[0.92, 1.00]$ are shown in the boxes. The event yield is normalized to 100 pb^{-1} at 10 TeV.

signal region.

With more data, we may fit the background isolation distribution from the data itself assuming some monotonically decaying probability distribution function for non-isolated electrons, floating parameters in the fit. Figure 13 shows the result of such a fit to "data" assuming a power law background distribution with the exponent floating in the fit. The result is consistent with the prediction based on shapes derived from QCD samples, but the statistical uncertainty is large due to limited statistics in the MC samples (e.g. the W+jets sample corresponds to 190 pb^{-1} of integrated luminosity).

9 Sideband Method: Fake Muons

The contribution of fake muons to the muon selection is in general lower than that for the electron selection. The primary sources of fake muons are shown in Figure 14. All the ideas about W+jets background estimation from the sideband of the isolation distribution apply to fake muons, but given their lower rate, it is possible to be more conservative in the background estimation without affecting the signal significance of the final result.

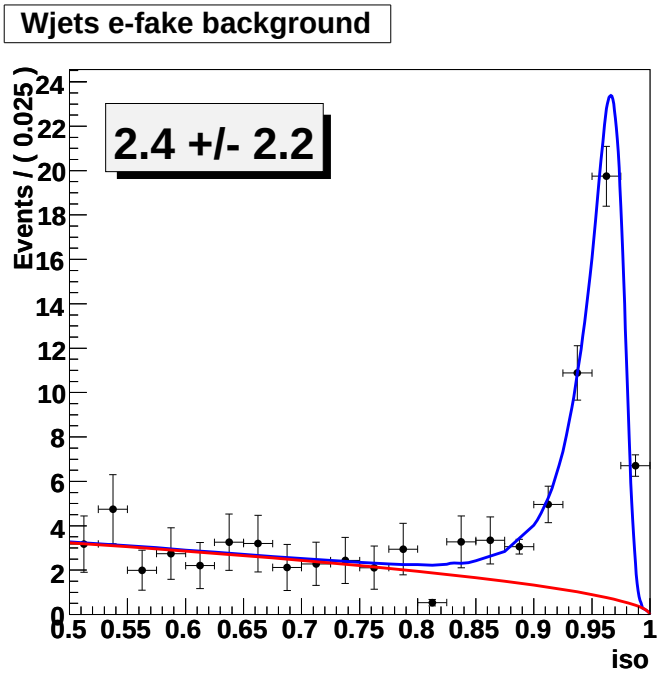

Figure 13: Unbinned maximum likelihood fit on the full sample of events. The pdf for the isolation in the signal region was extracted from $Z \rightarrow ee$ events. The background pdf floated in the fit. The red curve represents the background distribution. The W+jets background estimate due to fake electrons in the region $[0.92, 1.00]$ are shown in the boxes. The Event yield is normalized to 100 pb^{-1} at 10TeV.

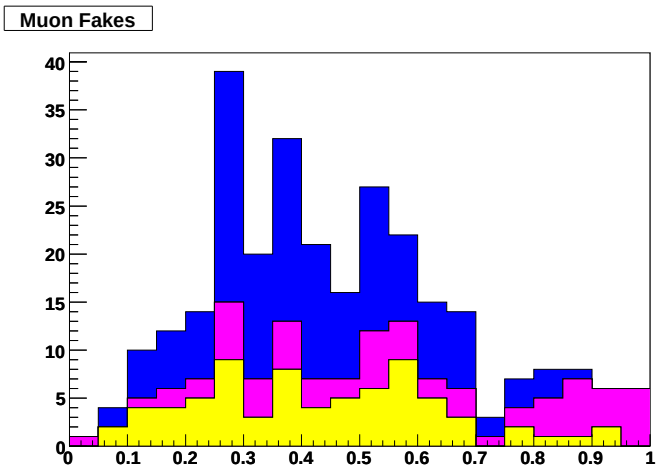

Figure 14: Shown are the relative isolation distributions for the dominant sources of fake muons for $W \rightarrow e\nu$ events: heavy quark semi-leptonic decays (blue), badly reconstructed global muons (magenta), all other sources (yellow). Events are weighted for $100pb^{-1}$ integrated luminosity at 10TeV.

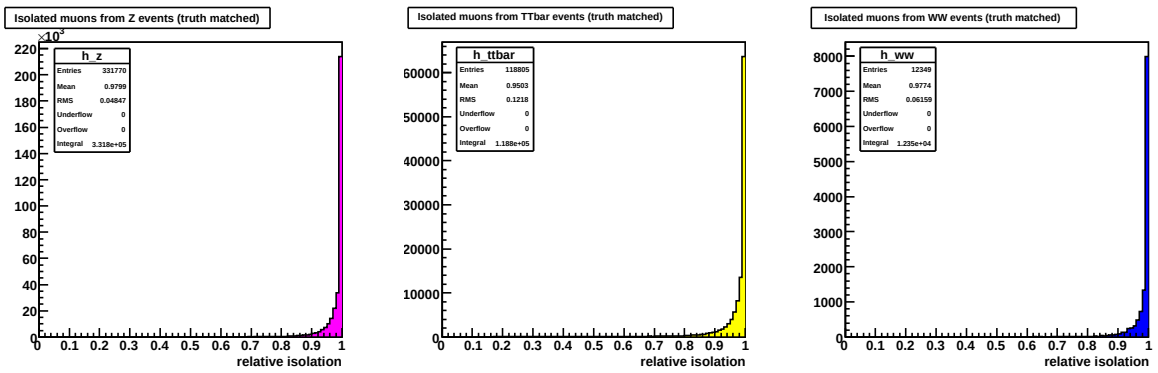

Figure 15: Shown are the relative isolation distributions for isolated muons from: $Z \rightarrow \mu\mu$ (magenta), $t\bar{t}$ (yellow) and WW (blue) events. Muons are truth matched to come from vector bosons and have standard selection requirements. The scale is arbitrary.

Among the various sources of fake muons, it is worth to highlight one of them - global muon fakes, which fail the tracker muon reconstruction requirements. The overall efficiency of the tracker muon reconstruction for true isolated muons reconstructed as global muons is more than 99%. Therefore it is worth to include in the muon selection requirements a requirement that the muon is reconstructed by both the global muon and the tracker muon algorithms. It is also worth to remove global muons with more than a 10% difference between the silicon tracker fit and the global muon fit, or to only use the silicon tracker fit results since no improvement in resolution is expected below 200 GeV.

In general the background estimation for fake muons from W+jets is similar to the electron one. Figure 15 shows isolation distributions for muons from vector bosons for WW, $t\bar{t}$ and Z events, which all look identical. Figure 16 shows isolation distributions for muons for different QCD samples, revealing the dependence of the background shape on the sample in use.

Following the procedure presented for the electron case, Figure 17 shows the expected background contribution from W+jets in the isolation region $[0.92, 1.0]$ for the $WW \rightarrow l\nu l\nu$ analysis (normalized to 100 pb^{-1}). The background distribution is fixed to that of QCD samples. Based on these fits, the expected W+jets background due to fake muons is estimated to be 0.2 ± 0.2 events.

10 Sideband Method: Comparison of predicted with observed fake leptons from W+jets in the WW Analysis

Combining the estimations for the electron and muon W+jets background contributions, 1.8 ± 0.4 events are predicted.

This prediction is reasonably consistent with the expected W+jets yield for the the WW analysis selection [1] of 4.7 ± 1.6 events in 100 pb^{-1}. A detailed examination of the nine Monte Carlo events on which this expectation is based shows that three of them are $W \rightarrow \mu\nu\gamma$. In these events the γ is emitted at a large angle, converts, and gives a reconstructed electron. The sideband method is not expected to capture these events. Thus, the prediction (1.8 ± 0.4 events) should really only be compared with 3.1 ± 1.3 W+jets events where one of the leptons comes from hadronic activity in the event.

11 Conclusion

Two data-driven methods to estimate the lepton fake contribution to di-lepton analyses of WW and $t\bar{t}$ were presented.

For the fake rate method, two-dimensional fake rates were extracted separately for electrons and muons using the inclusive QCD MC samples. The 2D fake rate allows to predict fake contributions to di-lepton signal selections both in shape and normalization. A closure test was performed to prove the absence of technical problems. This method was further validated using a W+jets MC sample which represents the main background from fake leptons for the di-lepton analyses under investigation. Recent MC samples (from the Summer08/Fall08 production) are severely limited in statistics. The comparison between observed and predicted fake leptons did not show any

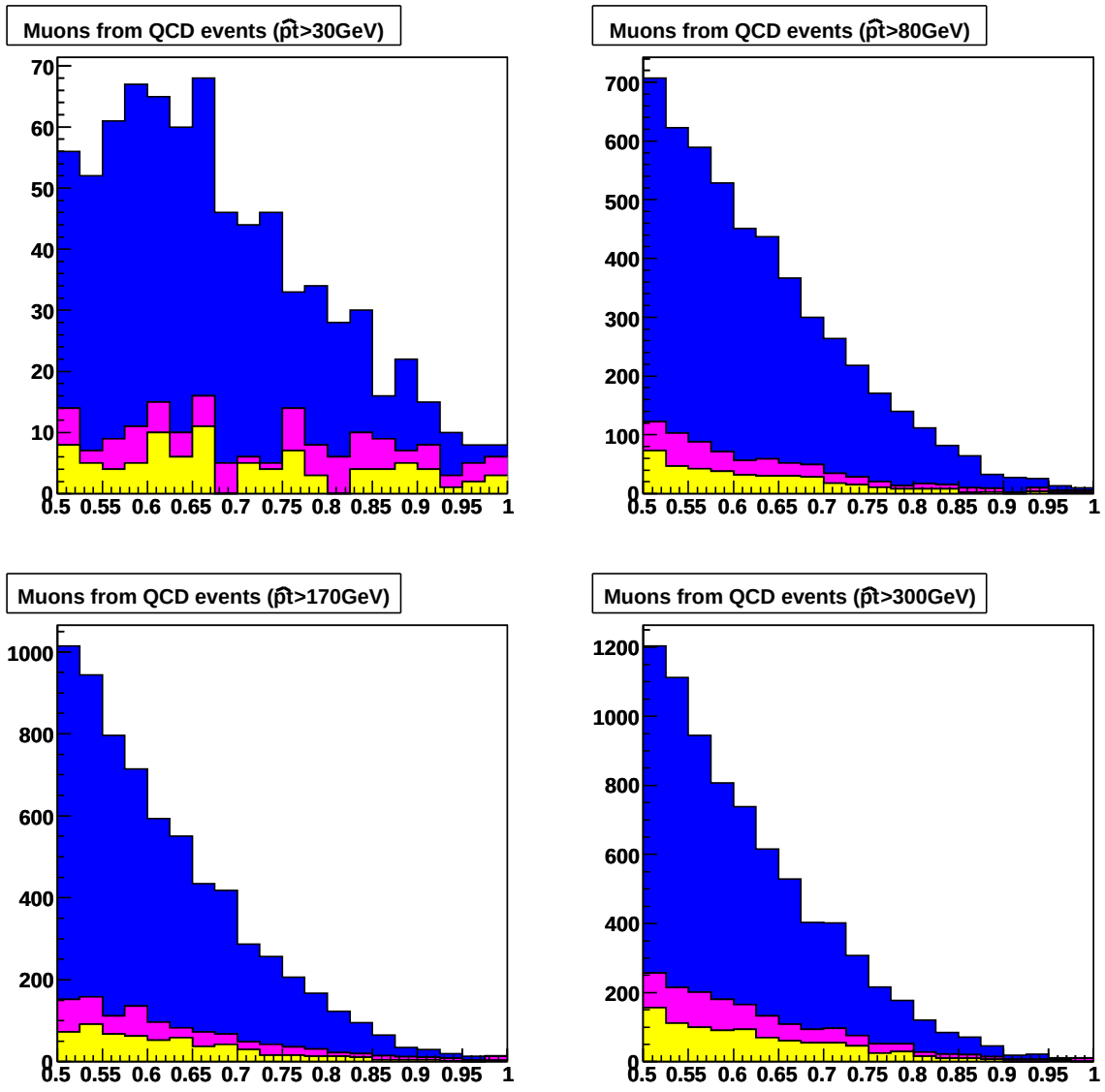

Figure 16: Shown are the relative isolation distributions for muons for different QCD samples. Each distribution is split into 3 categories: muons from heavy flavor semi-leptonic decays (blue), badly reconstructed global muons (magenta), all other sources (yellow). The scale is arbitrary.

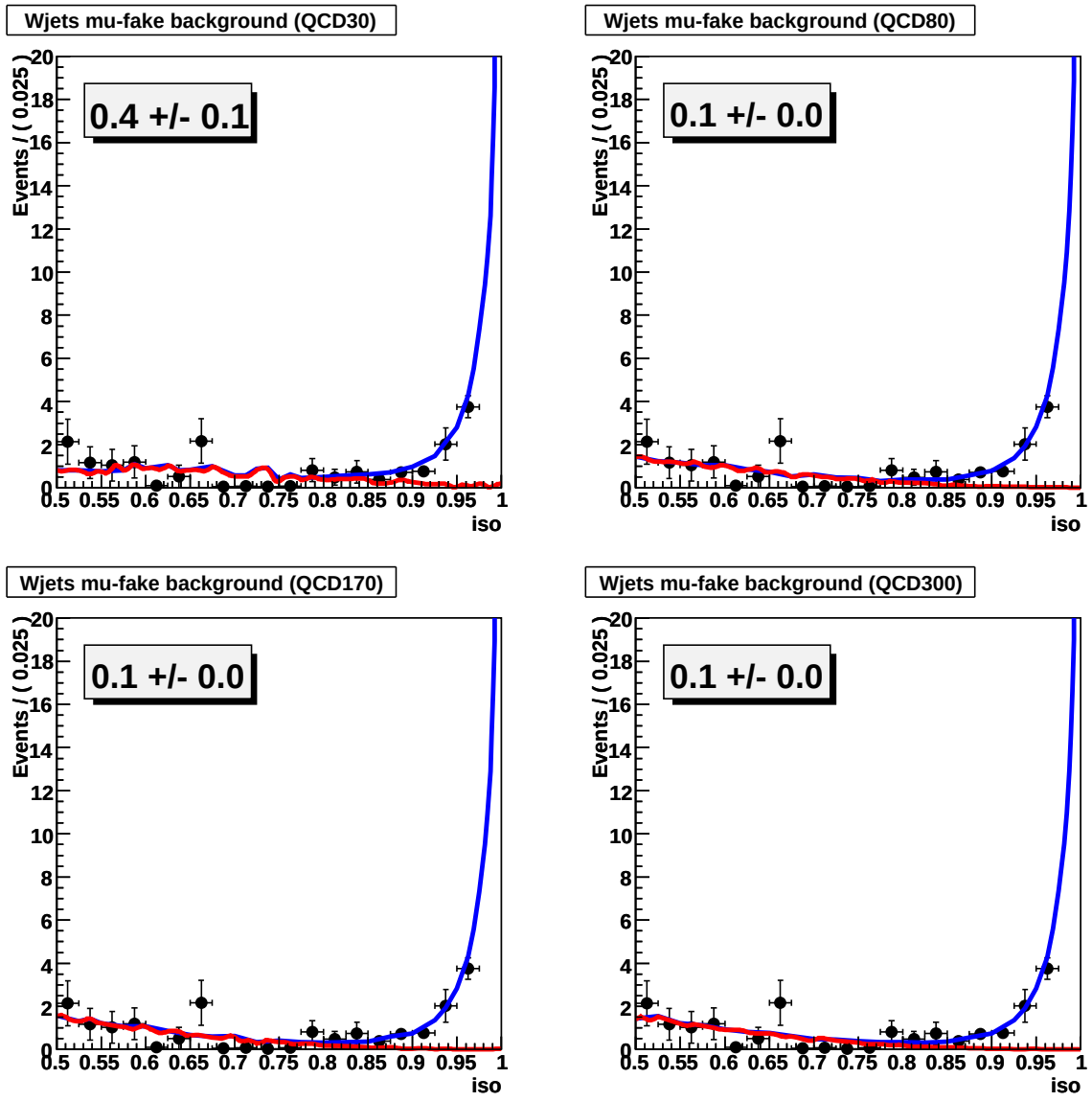

Figure 17: Unbinned maximum likelihood fit on the full sample of events. The signal pdf for the isolation distribution is extracted from $Z \rightarrow \mu\mu$ events and the background pdf is obtained from various QCD samples. The red curve represents the background distribution. The W+jets background estimates due to fake muons in the region $[0.92, 1.00]$ are shown in the boxes. The event yield is normalized to 100 pb^{-1} at 10TeV.

inconsistencies but did not allow for a statistically significant conclusion. The same studies performed previously using a high statistics W+jets sample (from the CSA07 production) showed very good agreement between observed and predicted electron fakes.

For the sideband method, isolation distributions for electron and muons were used to estimate fake contributions to the di-lepton analyses under investigation. By applying the sideband method to the full WW analysis selection, consistency between observed and predicted fake contributions in the W+jets sample was observed.

Therefore this note concludes that the presented data-driven methods to determine the fake lepton contributions to di-lepton analyses results in accurate predictions and can be used to estimate the fake contributions to WW and $t\bar{t}$ signals.

Using both methods provides a handle to estimate systematic effects of the lepton fake contribution estimation.

A WW Lepton analysis selection

A.1 Electron analysis selection

Electrons from the GSF electron collection are selected for the WW analysis using following cuts:

Cut	Selection
transverse momentum	$p_T^e \geq 20$ GeV
pseudo rapidity	$\lvert\eta_e\rvert \leq 2.5$
closest muon veto	$\Delta R_{e-\mu} > 0.1$
track+calo based isolation, see B.2	$p_T^e/(p_T^e + sumIso) > 0.92$
impact parameter	$\lvert d_0^e\rvert \leq 0.025$
electron identification	"category based tight category based tight", see App. F and [1]

Table 7: WW electron analysis selection.

A.2 Muon analysis selection

Global muons from the general muon collection are selected for the WW analysis using the following cuts:

Cut	Selection
transverse momentum	$p_T^\mu \geq 20$ GeV
pseudo rapidity	$\lvert\eta_\mu\rvert \leq 2.5$
track+calo based isolation, see B.2	$p_T^\mu/(p_T^\mu + sumIso) > 0.92$
number of tracker+μ-chamber hits	$n_{Hits} \geq 11$
global μ fit:	$\chi^2/NDoF \leq 10$
impact parameter	$\lvert d_0^\mu\rvert \leq 0.025$

Table 8: WW muon analysis selection.

B Isolation

Following isolation variables are used:

track isolation:

$$tkIso = \sum_{\Delta R=0.01}^{\Delta R=0.3} p_T^{track} \tag{2}$$

for tracks with $p_T^{min} \geq 1$ GeV, $n_{Hits}^{min} > 7$, $|d_0| < 0.1$ cm and $|z_0^l - z_0^{track}| < 0.5$ cm.

ECAL "jurassic" isolation:

$$ecalJuraIso = \sum_{\Delta R=0.05}^{\Delta R=0.4} E_{\mathrm{ECALCluster}} \sin(\theta_{\mathrm{Cluster}}) + \text{strip iso} \tag{3}$$

relative to electron position at ECAL excluding clusters where $|\eta_{Cluster} - \eta_{e\ at\ ECAL}| < 0.01$.

HCAL cone isolation:

$$hcalConeIso = \sum_{\Delta R=0}^{\Delta R=0.4} E_{HCAL\ Tower} + E_{HCAL\ Tower\ Outer\ Energy} \quad (4)$$

B.1 Track based isolation

The track based isolation is defined as:

$$p_T^l/(p_T^l + tkIso) > 0.92 \quad (5)$$

B.2 Track and calorimetry based isolation

The track and calorimetry based isolation is defined as:

$$p_T^e/(p_T^e + sumIso) > 0.92 \quad (6)$$

where

$$sumIso = tkIso + ecalJuraIso + hcalConeIso \quad (7)$$

C Logistics

The presented studies use two different sets of samples for determining the lepton fake rates and applying them to cross check their application.

There are two main sets of similar MC samples with large statistics. An initial one produced in 2007 identified by *CSA07* (using the 16X release of CMSSW for reconstruction) and one done in 2008 identified by *Summer08/Fall08* (using the 21X CMSSW release). The 2007 samples relevant for this study where significantly larger, especially the sample used to test the validity of the fake rate method (W+Jets). As the 2008 sample size is in fact so small that it does make stringent conclusions impossible, the validation strategy was chosen to be:

- Validate method using larger 2007 samples
- adjust Numerator and Denominator definitions to changes in reconstruction in CMSSW 21X/2008 samples to obtain similar selection performance as on 16X/2007 samples
- repeat validation in 21X
- if validation in 21X does not show obvious problems conclude that method is still valid, though based mainly on detailed tests done in the 2007 samples.

All samples are normalized to an integrated luminosity of $1 fb^{-1}$ using event weights taking into account the actual analyzed number of events.

C.1 Summer08 Samples for fake rate determination

Table 9 lists the Summer08 inclusive QCD MC samples which have been used for the lepton fake rate determination.

When combining the samples weighted according to the available luminosity, the first and second bin get the largest event weights, orders of magnitude larger than the following bins. Therefore, every statistical consideration is dominated by the first two bins. As a result, the available QCD statistics corresponds to order of 1 pb^{-1}.

These samples were generated, simulated and reconstructed in CMSSW_2_1_8 and were analyzed in CMSSW_2_2_3 using the following tags:

Sample	Luminosity $[pb^{-1}]$
/QCDpt30/Summer08_IDEAL_V9_v4/GEN-SIM-RECO	0.028
/QCDpt80/Summer08_IDEAL_V9_v2/GEN-SIM-RECO	1.551
/QCDpt170/Summer08_IDEAL_V9_v3/GEN-SIM-RECO	47.952
/QCDpt300/Summer08_IDEAL_V9_v1/GEN-SIM-RECO	818.641
/QCDpt470/Summer08_IDEAL_V9_v1/GEN-SIM-RECO	9508.321
/QCDpt800/Summer08_IDEAL_V9_reco-v4/GEN-SIM-RECO	251214.738

Table 9: Inclusive Summer08 QCD samples which have been used to extract the lepton fake rate.

- tag **V04-06-01** for package *TopQuarkAnalysis/TopObjectProducers*
- tag **V04-14-19** for package *PhysicsTools/PatAlgos*
- tag **V03-05-02** for package *PhysicsTools/PatUtils*
- tag **V03-18-04** for package *DataFormats/PatCandidates*
- tag **V01-06-06** for package *CondFormats/JetMETObjects*
- tag **V01-08-11** for package *JetMETCorrections/Configuration*
- tag **V02-09-00** for package *JetMETCorrections/Modules*
- tag **V01-07-11** for package *JetMETCorrections/Algorithms*
- tag **V03-02-06** for package *JetMETCorrections/JetPlusTrack*
- tag **V02-08-02-14** for package *RecoMET/METProducers/*
- tag **V02-05-00-16** for package *RecoMET/METAlgorithms/*
- tag **V00-06-02-09** for package *DataFormats/METReco/*
- tag **V00-04-02-15** for package *RecoMET/Configuration/*

(more information in [6]). The samples were generated with a lower $\hat{p}_T$ cut. To combine them, an upper $\hat{p}_T$ cut was applied on analysis level.

C.2 Fall08 Samples for tests of the fake rate

Table 10 lists the Fall08 W+jets MC sample which has been used for the lepton fake validation.

Sample
/WJets-madgraph/Fall08_IDEAL_V9_v1/GEN-SIM-RECO

Table 10: Fall08 W+jets samples which has been used to validate the lepton fake predictions.

The W+jets sample was generated, simulated and reconstructed in CMSSW_2_1_17 and analyzed in CMSSW_2_2_3 using the same additional tags listed in App. C.1.

C.3 CSA07 Samples for fake rate determination

Table 11 lists the CSA07 inclusive QCD MC samples are used for the lepton fake rate determination:

These samples were generated and simulated in CMSSW_1_4_X, reconstructed in CMSSW_1_5_X and re-reconstructed for the determination of the fake rates in CMSSW_1_6_12.

The used reconstruction differed from the released CMSSW_1_6_12 reconstruction in:

- tag **jet_corrections_16X_L5** for packages *CondFormats/JetMETObjects, JetMETCorrections/MCJet, JetMETCorrections/Modules*
- tag **eID16X_5Dic** for package *EgammaAnalysis/ElectronIDAlgos*

Sample
/QCD_Pt_0_15/CMSSW_1_5_2-CSA07-2047/GEN-SIM-DIGI-RECO
/QCD_Pt_15_20/CMSSW_1_5_2-CSA07-2026/GEN-SIM-DIGI-RECO
/QCD_Pt_20_30/CMSSW_1_5_2-CSA07-2162/GEN-SIM-DIGI-RECO
/QCD_Pt_30_50/CMSSW_1_5_2-CSA07-2048/GEN-SIM-DIGI-RECO
/QCD_Pt_50_80/CMSSW_1_5_2-CSA07-2049/GEN-SIM-DIGI-RECO
/QCD_Pt_80_120/CMSSW_1_5_2-CSA07-2027/GEN-SIM-DIGI-RECO
/QCD_Pt_120_170/CMSSW_1_5_2-CSA07-2171/GEN-SIM-DIGI-RECO
/QCD_Pt_170_230/CMSSW_1_5_2-CSA07-2069/GEN-SIM-DIGI-RECO
/QCD_Pt_230_300/CMSSW_1_5_2-CSA07-2050/GEN-SIM-DIGI-RECO
/QCD_Pt_300_380/CMSSW_1_5_2-CSA07-2061/GEN-SIM-DIGI-RECO
/QCD_Pt_380_470/CMSSW_1_5_2-CSA07-2172/GEN-SIM-DIGI-RECO
/QCD_Pt_470_600/CMSSW_1_5_2-CSA07-2096/GEN-SIM-DIGI-RECO

Table 11: Inclusive CSA07 QCD samples which have been used to extract the electron fake rate.

- tag **eID16X_26Nov** for package *EgammaAnalysis/ElectronIDProducers*
- tag **TQAF_168_080131** for packages *AnalysisDataFormats/TopObjects, TopQuarkAnalysis/Examples, TopQuarkAnalysis/TopEventProducers, TopQuarkAnalysis/TopEventSelection, TopQuarkAnalysis/TopJetCombination, TopQuarkAnalysis/TopJetSelection, TopQuarkAnalysis/TopKinFitter, TopQuarkAnalysis/TopLeptonSelection, TopQuarkAnalysis/TopObjectProducers, TopQuarkAnalysis/TopObjectResolutions, TopQuarkAnalysis/TopTools*

plus smaller differences (more information in [5]).

C.4 CSA07 Samples for tests of the fake rate

Until CMS records collision data, we tentatively use a W+jets sample to compare the lepton fake rate predictions to observed lepton fakes (see Sec. 6).

The W+jets sample was extracted from the samples listed in Table 12.

Sample
/CSA07Electron/CMSSW_1_6_7-CSA07-Chowder-A3-PDElectron-ReReco-100pb-Skims6-topDiLepton2Electron/USER
/CSA07Muon/CMSSW_1_6_7-CSA07-Chowder-A3-PDMuon-ReReco-100pb-Skims4-topDiLeptonMuonX/USER

Table 12: Electron and muon skims from CSA07 soup samples used to extract W+jets sample.

These samples were produced in the CSA07 challenge starting from a generation/simulation step in CMSSW_1_4_X. They have been combined in to a larger soup-like sample, reconstructed in CMSSW_1_6_X and skimmed with an electron and muon preselection [3].

The skims are re-reconstructed using the same CMSSW_1_6_12 reconstruction version used for the QCD samples (see. C.3). The double counting overlap between the two different skims is also taken care of by this step.

D Error treatment for prediction

The input is a fake rate and its statistical uncertainty as a function of η, p_T. To determine the error for a prediction, for example an n_{jet} distribution, one has to correctly account for correlated and uncorrelated statistical uncertainties in the fake rate.

The following code demonstrates the error determination adding correlated errors linearly and uncorrelated (bin-to-bin) errors in quadrature. We also added the statistical error of the n_{jet}.

```
// loop over events
for (iev; iev<nev; iev++) {

 // loop over FO, this event
```

```
 for (iFO; iFO<nFO; iFO++) {
      float thisFake = fake(eta,pt);
      float thisErr  = err(eta,pt);
      float thisWeight = blah;  // event weight

      // fill a 1D njet histogram
      // also fill a 3D (njet-eta-pt) histogram
      // to keep track of errors
        hnJet->Fill(njet, thisWeight*thisFake);
       hnJet3D->Fill(njet, eta, pt, thisWeight*thisErr);
  }
} // end loop over events

// Now fill the hnJet histogram with the appropriate error
// Correlated errors are added linearly (as kept track in the
// 3D histogram); uncorrelated errors (bin-to-bin) are added
// in quadrature
for (injet=0, injet<=nJetBin+1; injet++) {
 float err2 = 0;
 for (ieta=0; ieta<=netaBin+1; ieta++) {
   for (ipt=0; ipt<=nptBin+1; ipt++) {
     float dummy = hnJet3D->GetBinContent(injet,ieta,ipt);
     err2 = err2 + dummy*dummy;
   }
 }
 float err = sqrt(err2);
 hnJet->SetBinError(injet, err);
}
```

E Application test in CSA07

Using MC samples from the older MC production cycle (identified as CSA07 MC samples), events in which the W decays to a muon ($W + jets \rightarrow \mu + jets$) are used to test the validity of the MC QCD fake rate. As the W is known to decay to a muon, all remaining selected electrons are considered fake electrons.

As a general event selection, we require opposite-sign di-leptons with:

- $p_T^{lepton} \geq 20$ GeV
- $|\eta| \leq 2.4$
- using optimized MET cut as described in [2]

We thus define all objects satisfying the full electron selection (see Sec. 3) in truth-tagged $W \rightarrow \mu$ events as observed fake electrons.

We construct a prediction for these observed fake electrons by scaling all observed denominator objects (defined in 3) with the fake rate.

Figure 18 shows the distribution in transverse momentum and pseudo rapidity for the predicted and observed fake electrons. Agreement within the (still quite large) statistical errors[2)] is obtained.

Furthermore, predictions are obtained for objects not directly related to the fake objects. Figure 19 shows the distributions for the number of reconstructed jets and the missing E_T in W+jets events respectively. Good agreement is found also for these distributions.

[2)] For error treatment, see App. D.

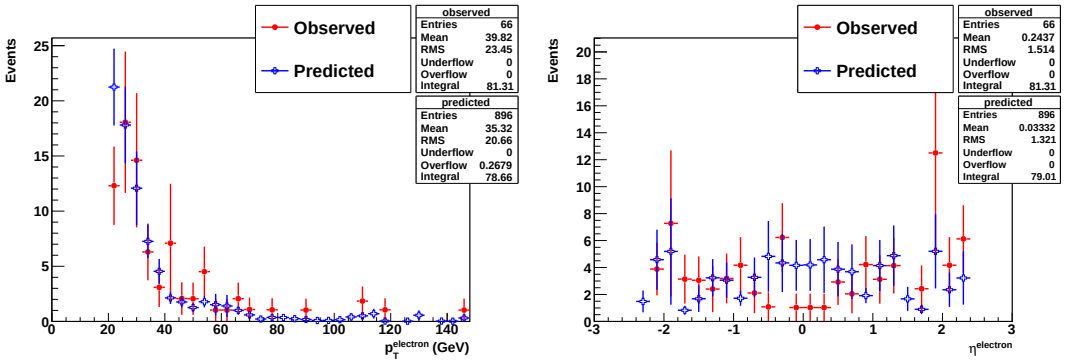

Figure 18: Comparison of the transverse momentum *(left)* and pseudo rapidity *(right)* distributions for fake electrons predicted by the fake rate (blue) with the observed fake electrons (red) in the full CSA07 W+jets sample. Distributions are scaled to 1 fb^{-1}.

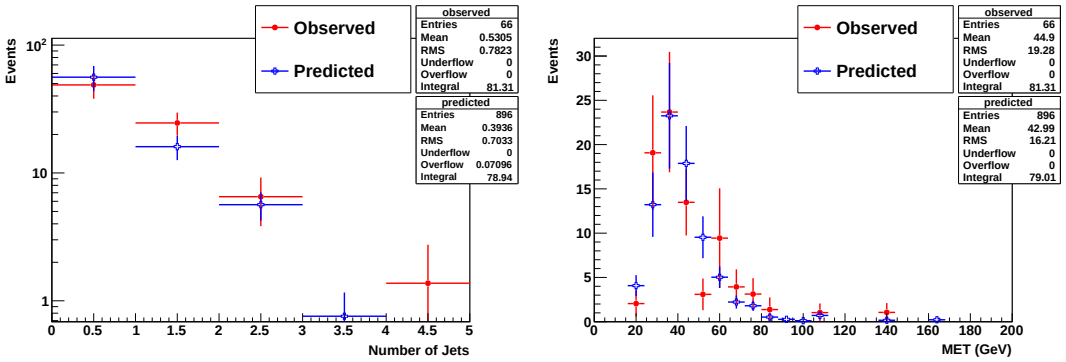

Figure 19: Comparison of the number of reconstructed jets *(left)* and missing E_T *(right)* in events containing fake electrons as predicted by the fake rate (blue) with the rate observed in events with fake electrons (red) in the full CSA07 W+jets sample. Distributions are scaled to 1 fb^{-1}.

F Electron selection details

To reject fake electrons, a standard category-dependent electron ID is applied [7]. The expected performance of this electron ID is described in [8]. The POG-recommended set of thresholds was optimized using `CMSSW_1_6_X`. In `CMSSW_2_2_X` some variables used in the selector have changed: H/E was changed to compute the HCAL E_T using the nearest HCAL tower to the super cluster and the log weighting factor used in $\sigma_{\eta\eta}$ was changed. Therefore the thresholds applied to these variables were updated in consultation with the E/gamma group [9].

The electron signature in the detector greatly depends on how much energy it radiates. We define the fractional energy loss to bremsstrahlung as determined by the track momentum $p_{\rm in}$ estimated at the interaction point and the track momentum $p_{\rm out}$ when the track exits the tracker.

$$f_{\rm brem} = \frac{p_{\rm in} - p_{\rm out}}{p_{\rm in}} \tag{8}$$

We require $E/p > \max[0.8, 0.9(1 - f_{\rm brem})]$, where E is the supercluster energy, p is the track momentum at the vertex.

Electrons are defined as being in the endcap if $|\eta| > 1.479$ and categorised according to their E/P and $f_{\rm brem}$ as follows.

- Category-0: $f_{\rm brem} > 0.06$ barrel (0.10 endcap) and $0.8 < E/P < 1.2$.
- Category-1: $f_{\rm brem} < 0.06$ barrel (0.10 endcap).
- Category-2 otherwise.

By cutting more tightly according to the expected signal to background ratio in each category, extra rejection power is possible compared to a simpler technique without categorisation. The variables used to distinguish between real and fake electrons are now described.

- H/E is the ratio of the E_T of the closest HCAL tower to the E_T of the electron reconstructed in the ECAL.
- $\sigma_{\eta\eta}$ is the covariance defined to be $\sum_i w_i(\eta_i - \bar{\eta}_{5\times5})^2/\sum_i w_i$ where $w_i = 4.7 + \ln(E_i/E_{5\times5})$.
- $\Delta\phi_{in}$ is the difference between the ϕ co-ordinate of the electron measured in the ECAL and the projection of the track as measured at the primary vertex and projected through the magnetic field to the ECAL.
- $\Delta\eta_{in}$ is the difference between the η co-ordinate of the electron measured in the ECAL and the projection of the track as measured at the primary vertex and projected to the ECAL.
- E_{seed}/P_{in} is the ratio of the energy of the seed cluster that initiated the bremsstrahlung recovery process to the momentum of the track at the vertex.

The variable $\sigma_{\eta\eta}$ was corrected for the η dependance of the crystal size in the endcap in the usual way by subtracting $0.2(|\eta| - 2.3)$ from the computed value. If E/P is greater than 1.5, then the $\Delta\phi_{in}$ threshold is loosened to 0.09 in the barrel region and 0.092 in the endcap region. The category dependent thresholds are tabulated in Tables 13, 14 and 15.

Table 13: Electron cuts for category-0, Bremming.

Parameter	Threshold (barrel)	Threshold (endcap)
H/E	< 0.041	< 0.034
$\sigma_{\eta\eta}$	< 0.0118	< 0.0271
$\Delta\phi_{in}$	< 0.032	< 0.025
$\Delta\eta_{in}$	< 0.0055	< 0.0060
E_{seed}/P_{in}	> 0.24	> 0.32

Table 14: Electron cuts for category-1, Low brem.

Parameter	Threshold (barrel)	Threshold (endcap)
H/E	< 0.028	< 0.012
$\sigma_{\eta\eta}$	< 0.0112	< 0.0263
$\Delta\phi_{in}$	< 0.016	< 0.035
$\Delta\eta_{in}$	< 0.0030	< 0.0055
E_{seed}/P_{in}	> 0.94	> 0.83

Table 15: Electron cuts for category-2, Bad track.

Parameter	Threshold (barrel)	Threshold (endcap)
H/E	< 0.025	< 0.016
$\sigma_{\eta\eta}$	< 0.0104	< 0.0256
$\Delta\phi_{in}$	< 0.0525	< 0.065
$\Delta\eta_{in}$	< 0.0065	< 0.0075
E_{seed}/P_{in}	> 0.11	N/A

References

[1] "A strategic plan for measuring the WW production cross section in pp collisions at $\sqrt{s} = 10$ TeV", note in preparation

[2] `https://twiki.cern.ch/twiki/bin/view/CMS/TWikiTopQuarkNotesSlava` (PAS TOP-08-01 and CMS AN/08-015).

[3] `http://www.hep.wisc.edu/~dasu/skimStatus.html`
`https://twiki.cern.ch/twiki/bin/view/CMS/DataOpsSamples`

[4] D. Glenzinski *et al.*, "The Fake Rate for the tight lepton and isolated track sample", CDF/DOC/TOP/CDFR/6524

[5] , "Patches to CMSSW_1_6_12,"

http://cmssw.cvs.cern.ch/cgi-bin/cmssw.cgi/UserCode/JRibnik/CMS2/Configuration/patchesToSource.sh.168tqaf?revision=1.1&view=markup&pathrev=V00-05-00

[6] , "Patches to CMSSW_2_2_3,"

http://cmssw.cvs.cern.ch/cgi-bin/cmssw.cgi/UserCode/JRibnik/CMS2/Configuration/patchesToSource.sh.223PAT?revision=1.6&view=markup&pathrev=V01-02-06

[7] TWiki: "Cut Based Electron ID"

https://twiki.cern.ch/twiki/bin/view/CMS/SWGuideCutBasedElectronID

[8] Talk: M. Sani, "Cut Based Electron ID"

http://indico.cern.ch/getFile.py/access?contribId=3&resId=0&materialId=slides&confId=22460

[9] Talk: M. Sani, "Retuning electron ID"

http://indico.cern.ch/contributionDisplay.py?contribId=0&confId=49643